

$^{131}\text{Sn}$  decay

H. Huck, M. L. Pérez, J. J. Rossi, and H. M. Sofía

*Departamento de Física, Comisión Nacional de Energía Atómica,**Av. del Libertador 8250, 1429 Buenos Aires, Argentina*

(Received 5 January 1981)

A level scheme for  $^{131}\text{Sb}$  is proposed taking into account the gamma-ray energy and intensity and the gamma-gamma coincidences obtained in the decay of  $^{131}\text{Sn}$ . The samples were obtained using on-line mass-separation techniques applied to  $^{235}\text{U}$  thermal-neutron fission products. The half-life of  $^{131}\text{Sn}$  was measured to be  $61 \pm 1$  s. The level structure in  $^{131}\text{Sb}$  is compared with a particle-core coupling calculation using a quadrupole proton-neutron interaction.

RADIOACTIVITY  $^{131}\text{Sn}$  (from  $^{235}\text{U}$  ( $n_{\text{th}}, f$ ); measured  $E_{\gamma}$ ,  $I_{\gamma}$ ,  $\gamma$ - $\gamma$  coincidences and  $T_{1/2}$  of  $^{131}\text{Sn}$ , Ge(Li), and Ge intrinsic detectors;  $^{131}\text{Sb}$  deduced levels and  $\beta$  branches. Mass-separated  $^{131}\text{Sn}$  and  $^{131}\text{Sb}$  activities.

## I. INTRODUCTION

The decay of  $^{131}\text{Sn}$  has been studied at the Buenos Aires (IALE) on-line isotope-separator facility as part of a systematic study of the short-lived Sn fission products and their daughters. The results of a study of the gamma-ray deexcitation following those decays and the level scheme deduced for  $^{131}\text{Sb}$  are presented.

The use of mass-separator on-line techniques in study of the  $^{131}\text{Sn}$  decay was reported by Schussler *et al.*,<sup>1</sup> who employed the Lohengrin facility at the high-flux reactor at the Institute Laue-Langevin (Grenoble) to obtain mass-separated  $^{131}\text{Sn}$  and used Ge(Li) detectors for gamma-ray spectroscopy and gamma-gamma coincidences. They deduced a level scheme for  $^{131}\text{Sb}$ , in which three gamma-ray transitions were placed among three excited levels and the ground state. Two beta-decaying isomers were observed by them in  $^{131}\text{Sn}$ , with half-lives of  $39 \pm 2$  and  $50 \pm 2$  s, in contrast to Izak and Amiel,<sup>2</sup> Fowler *et al.*,<sup>3</sup> and Grapengiesser *et al.*<sup>4</sup> who only observed one half-life of  $63 \pm 3$ ,  $65 \pm 6$ , and  $55 \pm 4$  s, respectively. The authors of Ref. 1 also determined the half-life of the 1676-keV level of  $^{131}\text{Sb}$  to be 50  $\mu\text{s}$ .

In the present work a new level scheme for  $^{131}\text{Sb}$  is presented. This level scheme was deduced from the gamma-ray energies and intensities, and gamma-gamma coincidences measurements. The

ground-state beta branching in the decay of  $^{131}\text{Sn}$  was deduced from measurement of the transition intensities to the  $^{131}\text{Te}$  ground state and use of the independent yields of  $^{131}\text{Sn}$  and  $^{131}\text{Sb}$  in the thermal fission of  $^{235}\text{U}$ .<sup>3</sup>

In Sec. IV the data are discussed in terms of a coupling of a single proton state to a pairing vibrational core.

## II. EXPERIMENTAL PROCEDURES AND RESULTS

## A. Experimental arrangement of the on-line system for production and collection of samples

The  $^{131}\text{Sn}$  activity was obtained as a thermal-fission product of  $^{235}\text{U}$ . The fissioning uranium sample was in the form of  $\text{UO}_2$ , which was incorporated into the ion source<sup>5</sup> of the isotope separator of the IALE project and exposed to a thermal neutron flux of approximately  $5 \times 10^8 \text{ n/cm}^2 \text{ s}$ . The mass 131 beam is received on a moving tape collector at the focus of the isotope separator. No contaminations from other masses were observed.

Ge(Li) and Ge(Hp) detectors were placed immediately outside the walls of the tape collector. A more complete description of the isotope separator system is available in the literature.<sup>6</sup> The collector assembly was operated with different time schedules to vary the Sn to Sb activity ratio, and

thus allow a positive assignment for the detected radiations.

### B. Gamma-ray measurements

1. *Singles gamma-ray spectra.* A Ge(Li) detector of 95 cm<sup>3</sup>, a Ge(Hp) detector of 65 cm<sup>3</sup>, and a Ge(Li) detector, produced in our laboratory, having 45 cm<sup>3</sup> were used to record the gamma spectra. When operated for short periods, and at an overall gain of 0.33 keV/channel, the resolutions for the 1.33-MeV <sup>60</sup>Co gamma ray were 1.85, 1.95, and 2.5 keV, respectively. The detector pulses were fed (through conventional electronics) to a 4096-channel analyzing system provided with a small computer.

Energy calibrations were made using the lines of the <sup>60</sup>Co, <sup>57</sup>Co, <sup>88</sup>Y, <sup>203</sup>Hg standards<sup>7</sup> and the gam-

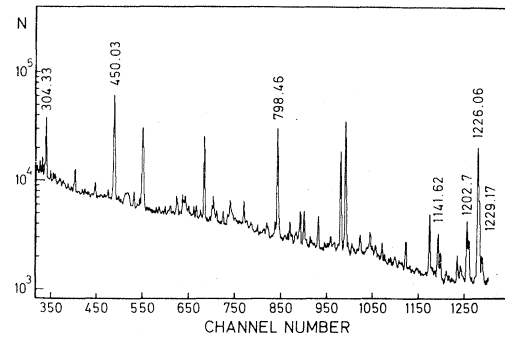


FIG. 1. A gamma-ray spectrum of the  $A = 131$  isobars, measured to enhance activities with 61 s half-life. The recording was made in 1 h.

ma ray from the  $H(n,\gamma)d$  reaction. Efficiency calibrations over the range 0.13–3.3 MeV were performed by collecting  $A = 138$  activity on line, with

TABLE I. Gamma rays from <sup>131</sup>Sn.

$E_\gamma$ (keV)	(a)	Relative intensity		Coincidence gamma-rays (keV)	Transition	
		(a)	(a)		$E_f$	$E_i$
62.9	0.2	1.5	0.5			
82.29	0.06	21.0	3.0			
108.8	0.3	1.0	0.7			
118.06	0.15	2.8	0.7			
155.9	0.6	1.4	0.5			
190.73 <sup>b</sup>	0.13	8.0	1.0			
197.8	0.2	2.4	0.5			
203.2	0.5	1.0	0.5			
208.25	0.30	1.4	0.5			
213.9	0.2	2.6	0.5			
217.15	0.13	2.5	0.5			
223.70	0.25	1.4	0.4			
240.43 <sup>b</sup>	0.07	6.5	1.0	999.8	1676	1931
251.70 <sup>b</sup>	0.10	4.6	0.8	314.4, 430.6, 793.5, 1182.4, 1229.2	1229	1482
260.15	0.40	1.0	0.5			
266.89	0.21	2.0	0.5			
285.0	0.2	3.0	0.9			
304.33 <sup>b</sup>	0.03	32.0	4.0	885.1, 1141.2, 1328.4	1676	1980
314.45 <sup>b</sup>	0.13	2.8	0.6	251.7, 1182.4	2663	2977
320.75	0.12	3.4	0.6			
331.7	0.6	0.8	0.4			
359.60	0.35	0.8	0.4			
367.40 <sup>b</sup>	0.05	7.6	1.1			
383.2	0.3	1.3	0.3			
387.6	0.4	1.3	0.4			
410.25 <sup>b</sup>	0.20	5.1	1.0	774.7	1666	2086
430.6	0.6	1.0	0.5			
450.03 <sup>b</sup>	0.05	90.0	10.0	1226.0	1226	1676
504.6	0.3	2.9	0.9			

TABLE I (Continued).

$E_\gamma$ (keV)	(a)	Relative intensity	(a)	Coincidence gamma-rays (keV)	Transition	
					$E_f$	$E_i$
583.5 <sup>b</sup>	0.2	5.2	1.0	1229.2	1229	1812
682.4 <sup>b</sup>	0.3	3.1	0.9	798.5, 1182.4, 1787.5	798	1481
692.3	0.2	4.1	1.0			
774.70	0.16	3.5	0.6	410.3	2086	2860
793.5	0.2	3.7	1.2	1481.1	1481	2274
798.50 <sup>b</sup>	0.02	86.0	10.0	430.6, 682.4, 1073.4, 1182.4, 1202.6, 1593.6, 1762.6, 2186.4, 2470.5	0	798
801.63	0.26	1.4	0.3			
815.3	0.3	4.4	1.2			
885.08 <sup>b</sup>	0.07	8.9	1.2	304.3	1980	2865
898.5	0.4	1.4	0.5			
904.6	0.7	1.0	0.3			
999.8	0.3	4.3	1.1	240.4	1916	2916
1022.1 <sup>b</sup>	0.2	4.0	1.0	1931.1	1931	2954
1036.9	0.9	0.7	0.4			
1073.36 <sup>b</sup>	0.12	8.6	1.4	314.4, 798.5, 1202.6	798	1872
1141.2	0.2	2.5	0.5	304.3	1980	3121
1141.6 <sup>b</sup>	0.2	10.0	2.0	314.4, 1250.7, 1836.3, 1918.9	0	1141
1182.4 <sup>b</sup>	0.2	4.2	1.0	251.7, 682.4, 798.5, 1481.1	1481	2663
1202.6	0.2	4.0	2.0	798.5, 1073.4	1872	3075
1202.6 <sup>b</sup>	0.2	15.0	3.0	1775.6	0	1202
1226.03 <sup>b</sup>	0.03	100.0	10.0	450.0, 504.6, 1894.3	0	1226
1229.23 <sup>b</sup>	0.006	30.0	3.5	251.7, 583.5, 1724.9	0	1229
1236.3	0.4	4.1	1.0			
1250.7	0.7	1.2	0.5			
1328.03	0.18	3.3	0.6			
1375.7	0.5	1.3	0.5			
1481.12 <sup>b</sup>	0.08	12.0	1.5	793.5, 1182.4, 1787.5	0	1481
1496.4	0.3	2.2	0.3			
1593.6 <sup>b</sup>	0.2	2.9	0.7			
1639.7	0.5	1.6	0.4			
1724.90	0.26	2.7	0.7	1229.2	1229	2954
1736.5	0.7	1.0	0.5			
1762.60	0.25	3.0	0.8			
1775.60	0.18	3.9	0.8	1202.6	1202	2973
1787.47	0.18	4.4	0.8	1481.1	1481	3268
1836.31 <sup>b</sup>	0.16	3.6	0.9	1141.6	1141	2977
1872.6	0.5	1.3	0.4			
1890.4	0.9	1.4	0.3			
1894.25 <sup>b</sup>	0.40	2.2	0.5	1226.6	1226	3112
1918.85	0.50	1.4	0.3			
1931.05 <sup>b</sup>	0.08	9.2	2.0	1022.1	0	1931
1942.6	0.4	1.6	0.4			
1951.2	0.5	1.5	0.4			
2003.4	0.5	1.2	0.3			
2029.30	0.17	5.4	1.0			
2039.25	0.25	4.2	1.0			
2082.45 <sup>b</sup>	0.20	4.7	1.2			
2092.8	0.3	2.3	0.6			
2121.5	0.6	1.2	0.3			
2150.4	0.7	2.6	0.7			
2186.4	0.2	4.0	1.0			

TABLE I. (Continued.)

$E_\gamma$ (keV)	(a)	Relative intensity	(a)	Coincidence gamma-rays (keV)	Transition	
					$E_f$	$E_i$
2208.95	0.20	3.4	1.0			
2470.5	0.4	3.3	0.8			
2614.4	0.4	2.6	0.8			
2722.0	0.4	1.6	0.4			
2833.9	0.6	1.0	0.4			
2977.7	0.4	1.2	0.3			
3267.5	0.7	3.3	0.8			
3367.0	0.8	1.7	0.4			
3412.3	0.9	1.0	0.3			

<sup>a</sup>Errors.

<sup>b</sup>Already observed by Schussler *et al.* (Ref. 1).

the same geometry as that used for the  $A = 131$  measurements, and recording the standard  $^{138}\text{Xe}$  and  $^{138}\text{Cs}$  decay lines.<sup>8</sup> The low-energy region was calibrated using  $^{57}\text{Co}$  and  $^{241}\text{Am}$  standard sources. The resulting efficiency curves were defined within  $\pm 7\%$  for the 0.2–2.5 MeV range and  $\pm 10\%$  for the 0.05–0.2 and 2.5–4.0 MeV ranges. Spectra were analyzed by computer methods using the AN-PIK program<sup>7</sup> developed for use in our small computer and the energy calibration was performed with the CALIB program.<sup>7</sup>

Figure 1 shows a typical on-line gamma spectrum, where the  $^{131}\text{Sn}$  activity is enhanced with respect to  $^{131}\text{Sb}$  by an appropriate sequence for the moving-tape collection time. Several runs, with different enhancements, allow a positive identification for the origin of the transitions through spectra comparison. The results are summarized in Table I. They are in general agreement with the scarce data previously reported.<sup>1</sup> We were able to assign 90 transitions to the  $^{131}\text{Sn}$  decay.

2. *Gamma-gamma coincidences.* The 95 cm<sup>3</sup> and the 45 cm<sup>3</sup> Ge(Li) detectors were used for the gamma-gamma coincidence measurements. The resolving time of the coincidence circuit was 100 ns. Coincidence events were stored as 4096  $\times$  4096 bidimensional data using a magnetic-tape buffer, as described in Ref. 9.

A run of  $10^7$  events of gamma-gamma coincidences was made while cycling the moving-tape collector, each 6 min in order to obtain saturated activity of  $^{131}\text{Sn}$  and to keep the  $^{131}\text{Sb}$  and  $^{131}\text{Te}$  activities at a negligible level. No random coincidences were subtracted, because sample activity was kept sufficiently low. The efficiency of the coincidence circuit was unity between 150–2500

keV. The gamma-gamma coincidences results are summarized in Table I and Fig. 2 shows the coincidences with the 798-keV gate.

3. *Lifetime.* Ground-state half-lives were measured with the 95-cm<sup>3</sup> Ge(Li) detector using the spectrum-multiscaling technique for the intense gamma peaks between 250 and 1300 keV. The half-life for the 304-, 450-, 798-, and 1226-keV gamma rays in the decay of  $^{131}\text{Sn}$ , was determined (Fig. 3) to be  $61 \pm 1$  s, in agreement with Refs. 2–4, and in partial agreement with Ref. 1. The experimental discrepancy with the 798-keV transition cannot be explained easily since, on one hand, both in Ref. 1 and in the present works, the activi-

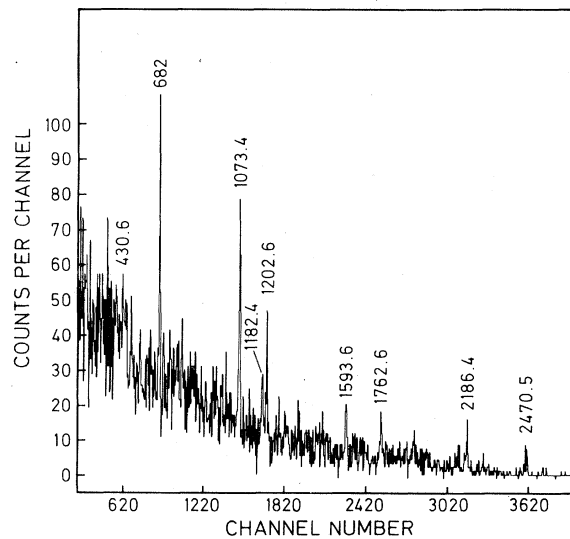


FIG. 2. Typical coincidence spectrum with gate of 798 keV.

ties have been produced by the same method (thermal neutron, U fission). On the other hand, the extraction techniques differ (recoil and diffusion, respectively), and one would expect this fact to produce differences in the relative populations of the Sn isomers obtained. One possible explanation may be the existence of an undetected transition between the two Sn isomers, and that we thus see the short decay fed by the long half-life, strongly present because of our relatively slow extraction method. In Ref. 1 the short isomer should be fed mainly through the  $^{131}\text{In}$  (approximately 0.3 s) decay. However, the relative intensities we obtained for the 798- and 1226-keV gamma rays are in reasonable agreement with those reported in Ref. 1. This would not be expected if that study was significantly influenced by the presence of  $^{131}\text{In}$  decays, but a particular combination of their experimental conditions and the relative populations of  $^{131}\text{In}$ ,  $^{131}\text{Sn}$ , and  $^{131}\text{Sn}^m$  may yield similar relative gamma intensities. On the other hand, the existence of two isomers in  $^{131}\text{Sn}$  is necessary in order to explain the characteristics of the proposed level scheme.

### III. LEVEL SCHEME

The level scheme proposed for the  $^{131}\text{Sn}$  decay is shown in Fig. 4. It has been built using the experimental results reported in Sec. II and contains 67 transitions that carry 90% of the observed gamma intensity within a scheme of 36 levels. The gamma rays of 1141 and 1202 keV are placed twice by coincidences and their intensities are divided proportionately to the coincidence intensities.

All the levels, except the 1758, 1866, 2043, 3367, and 3412 keV are supported by gamma-gamma coincidence results, energy sums, and intensity relations. The levels at 3367 and 3412 keV are built only on the basis of energy sums and intensity relations using the NIVEL program.<sup>7</sup>

The half-life of 50  $\mu\text{s}$  for the 1676-keV level reported by Schussler *et al.*<sup>1</sup> allows us to place the pairs of coincidences 304-885 keV, 304-1141 keV, 304-1328 keV, 240-999 keV, 410-774 keV, and the relatively intense 82-, 190-, and 367-keV gamma rays, which are not present in coincidences, above that level. In consequence, the beta feeding to the 1676 keV level is approximately zero.

The values of Schussler *et al.*<sup>1</sup> for the spins and parities agree with the odd-Sn systematics and, therefore, we adopt  $\frac{7}{2}^+$  for the ground-state and

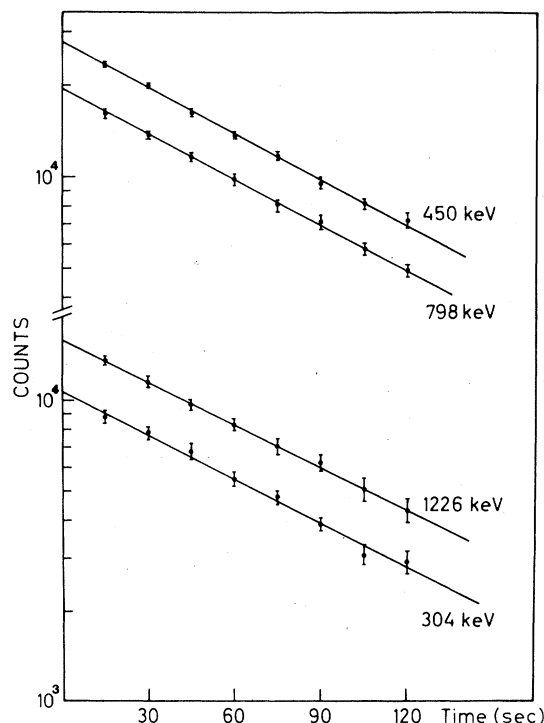


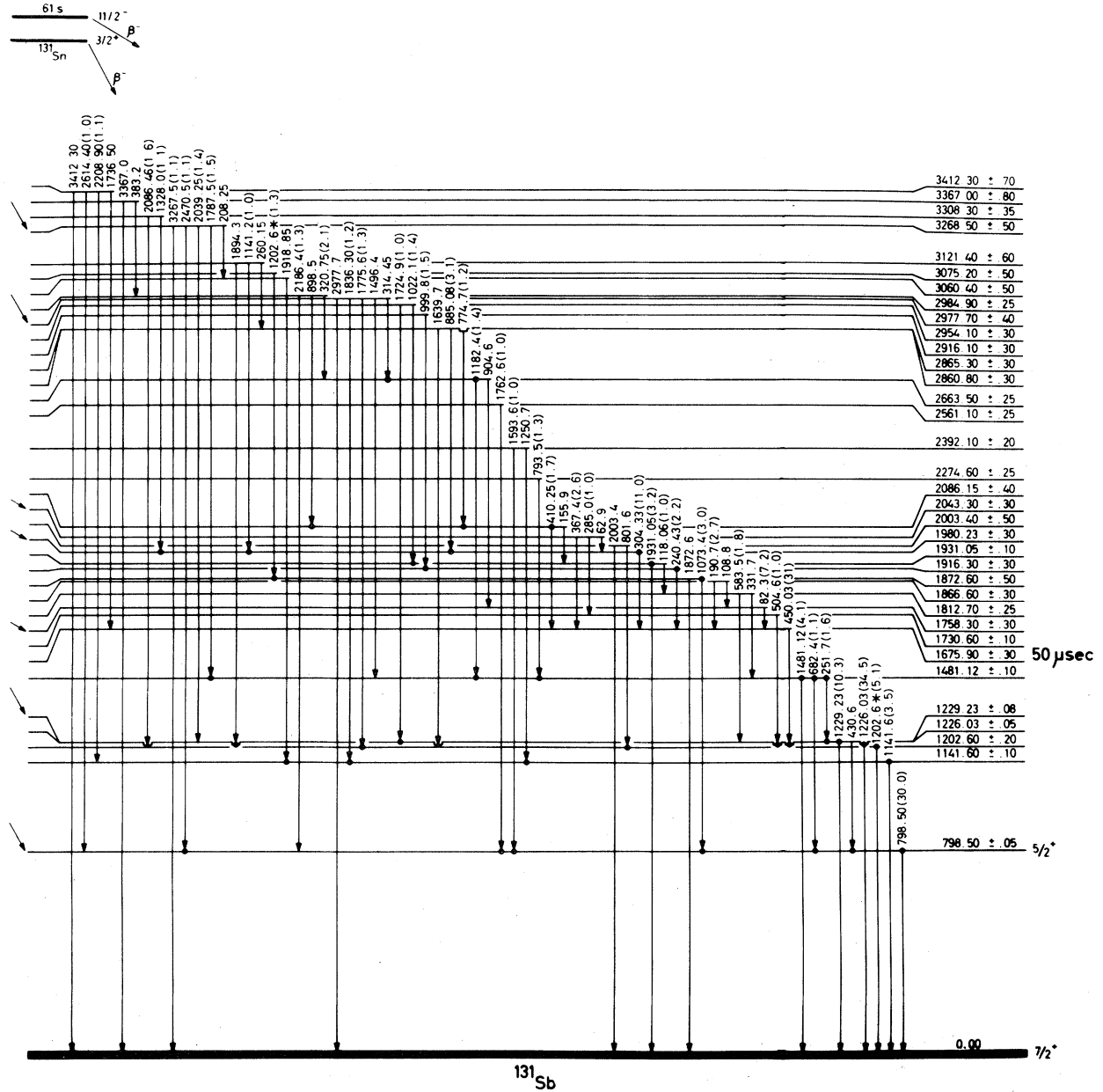
FIG. 3. Decay curves of the most important gamma transitions in the 250–1300 keV range.

$\frac{5}{2}^+$  for the first excited level.

In the range of 1140–1224 keV there are four levels, whose structure may be expected to be like that of the doublets 1114.3-1095.6 keV in  $^{127}\text{Sb}$  (Ref. 10) and 1164.3-1128.4 keV in  $^{129}\text{Sb}$  (Ref. 11), that have possible assignments  $(\frac{9}{2}^+, \frac{11}{2}^+)$ . Thus we suggest spin  $\frac{11}{2}^+$  for the 1226-keV level, which is consistent with its observed feeding from the 1676-keV level for which Schussler *et al.*<sup>1</sup> have proposed spin  $(\frac{15}{2}^-)$ .

It is meaningless to propose  $\log ft$  values in view of the assumption of two different parents, strongly suggested by the possible beta feedings calculated from gamma-intensity balances, taking into account the different possible  $J, \pi$  assignments discussed earlier. The strongest beta feedings are drawn in Fig. 4 showing their most plausible origin.

The beta branch to the ground state has been calculated as  $6 \pm 4\%$ , taking into account the total gamma intensity of the Sn decay and the one of the Sb decay, and comparing them with the predicted fission yields, with corrections due to the different half-lives and different yields in our on-line system.

FIG. 4. The decay scheme of  $^{131}\text{Sn}$  as obtained in this work.

## IV. DISCUSSION

The results can be discussed in terms of particle-core coupling calculations. The core ( $^{130}\text{Sn}$ ) can be described microscopically as a collective two-hole state coupled to  $0^+$  (ground state) or  $2^+$  (first excited state). Thus, these states can be thought of as multipole pairing vibrations of the doubly magic  $^{132}\text{Sn}$ .<sup>12</sup> The multipole pairing modes can be produced by a separable pairing in-

teraction, which is a schematic representation of the short-range nucleon-nucleon force.

$$H_p = -G_\lambda \pi(2\lambda + 1) \sum_\mu P_{\lambda\mu}^\dagger P_{\lambda\mu}, \quad (5.1)$$

where

$$P_{\lambda\mu}^\dagger = -\frac{2}{2\lambda + 1} \sum_{j_1 \geq j_2} \langle j_1 || \Omega^\lambda Y_\lambda || j_2 \rangle \frac{[C_{j_1}^\dagger C_{j_2}^\dagger]_\mu^\lambda}{1 + \delta_{j_1 j_2}}. \quad (5.2)$$

TABLE II. Single particle and pairing-vibration energies used in the particle-core theoretical calculations.

Neutron states	Energies (MeV)	Proton states	Energies (MeV)	Collective pairing vibrations	Energies (MeV)
$2d_{5/2}$	1.09	$1g_{7/2}$	0.0	$0^+$	0.0
$1g_{7/2}$	1.815	$2d_{5/2}$	0.798	$2^+$	1.217
$3s_{1/2}$	2.341				
$1h_{11/2}$	3.546				
$2d_{3/2}$	3.750				

The operator  $C_j^\dagger$  creates a particle in an orbital  $j$ . This force was diagonalized for  $\lambda=0, 2$  in the Tamm-Dancoff approximation and in a basis given by two holes in the single particle levels below the 82 magic closed shell (Table II). The coupling constant  $G_\lambda$  was fixed by fitting the experimental binding energy of the lowest state with spin  $\lambda$ .

The energy spectrum of <sup>131</sup>Sb has been calculated by coupling the single proton states (Table II) to the pairing vibrations of the <sup>130</sup>Sn core through a quadrupole proton-neutron interaction.

$$H_Q = -\frac{\chi}{2} \sum_{\mu} (Q_{\mu}^{\dagger})_{\pi} (Q_{\mu})_{\nu} + (Q_{\mu}^{\dagger})_{\nu} (Q_{\mu})_{\pi}, \quad (5.3)$$

where  $(Q_{\mu})_{\pi}$  [ $(Q_{\mu})_{\nu}$ ] are the proton (neutron) quadrupole particle-hole operators.

$$Q_{\mu} = -\frac{1}{\sqrt{5}} \sum_{j_1 j_2} \langle j_1 || r^{\lambda} Y_{\lambda} || j_2 \rangle \left[ C_{j_1}^{\dagger} C_{j_2} \right]_{\mu}^{\lambda}. \quad (5.4)$$

Within the nuclear field theory<sup>13</sup> framework, the matrix elements of  $H_Q$  have been worked out to first order in a basis of a single proton coupled to the  $0^+$  and  $2^+$  modes of <sup>130</sup>Sn. The strength of the interaction  $\chi$  has been used as a free parameter to fit the experimental data. The theoretical results are shown in Fig. 5 in comparison with the experimental ones. Previous theoretical descriptions have been attempted in this region<sup>14</sup> using particle core (<sup>127</sup>Sb) and shell model (<sup>131</sup>Sb) calculations. In Ref. 14 a surface vibrator is assumed for the core, different from our pairing (two holes) collective states  $0^+$  and  $2^+$  in <sup>130</sup>Sn.

Our theoretical description predicts a multiplet composed of the  $g_{7/2}$  proton state coupled to the  $2^+$  collective state in <sup>130</sup>Sn at about 1220 keV, which explains the set of states that appears at this energy in <sup>131</sup>Sb. (Reference 14 also predicts a mul-

tiplet at this energy, but the ordering of the states is slightly different.) In particular, the  $\frac{11}{2}^+$  state of the multiplet is fed by a 450-keV gamma ray from a state with a measured 50  $\mu$ s half-life. The angular momentum and parity of this last state was assumed in Ref. 1 to be  $\frac{15}{2}^-$  in agreement with the lifetime of the observed electromagnetic transition to the  $\frac{11}{2}^+$ .

It is worthwhile to mention that the observed

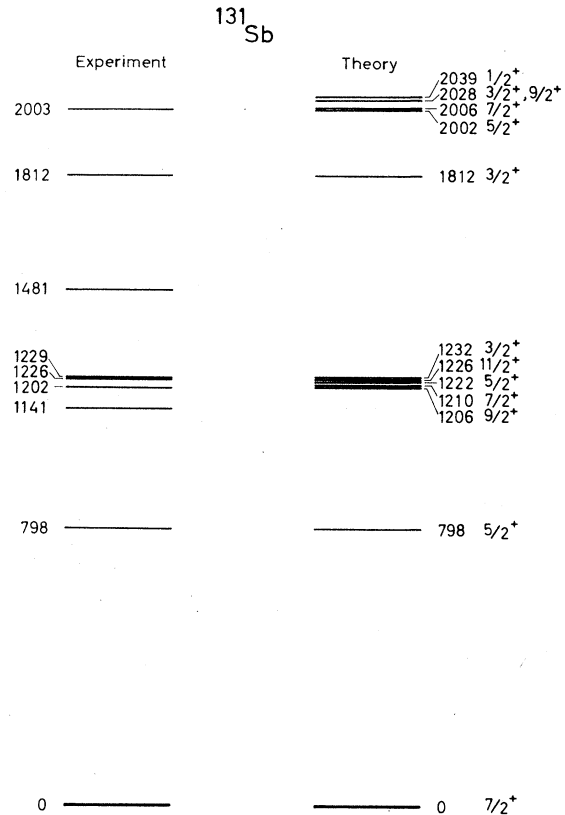


FIG. 5. Tentative angular momentum and positive parity assignment to some experimental levels for <sup>131</sup>Sb<sub>80</sub> from a nuclear field theory calculation.

data in odd Sn nuclei<sup>10</sup> show two isomeric states corresponding to the neutron states  $d_{3/2}$  and  $h_{11/2}$ . As discussed previously, Schussler *et al.*<sup>1</sup> reported two half-lives for <sup>131</sup>Sn. In this work, however, only one half-life ( $61 \pm 1$  s) has been observed. The existence of two parent states in <sup>131</sup>Sn would explain some features of the beta transitions which could not be otherwise explained. A  $d_{3/2}$  parent state would have allowed beta decay to the 798-

keV level, if the latter level is assumed to be a  $d_{5/2}$  proton state coupled to the <sup>130</sup>Sn ground state, in agreement with the systematic data observed in the odd Sb. In addition a  $h_{11/2}$  parent state would explain the existence of the feeding of the high-spin levels decaying to the  $\frac{15}{2}^-$  at 1676 keV. Experimental evidence for the existence of two parent states in <sup>131</sup>Sn will be the object of a more detailed experimental study.

<sup>1</sup>F. Schussler, J. Blachot, J. P. Bocquet, and E. Monand, *Z. Phys. A* **281**, 229 (1977).

<sup>2</sup>T. Izak and S. Amiel, *J. Inorg. Nucl. Chem.* **34**, 1469 (1972).

<sup>3</sup>M. M. Fowler, G. W. Goth, C. C. Lin, and A. C. Wahl, *J. Inorg. Nucl. Chem.* **36**, 1191 (1974).

<sup>4</sup>B. Grapengeisser, E. Lund, and G. Rudstam, *J. Inorg. Nucl. Chem.* **36**, 2409 (1974).

<sup>5</sup>H. Huck, J. Orecchia, M. L. Pérez, J. J. Rossi, A. Tergigni, and J. Vidallé (unpublished).

<sup>6</sup>E. Achterberg, F. C. Iglesias, A. E. Jech, A. Kasulin, E. Kerner, J. Mónico, J. A. Moragues, D. Otero, M. L. Pérez, M. Pinamonti, A. N. Proto, R. Requejo, J. J. Rossi, W. Scheuer, and J. F. Suárez, *Nucl. Instrum. Methods* **101**, 555 (1972).

<sup>7</sup>E. Achterberg, thesis, 1979 (unpublished).

<sup>8</sup>E. Achterberg, F. C. Iglesias, A. E. Jech, J. A. Moragues, D. Otero, M. L. Pérez, A. N. Proto, J. J. Rossi, and W. Scheuer, *Nucl. Instrum. Methods* **116**, 453 (1973).

<sup>9</sup>E. Achterberg, F. C. Iglesias, A. E. Jech, J. A. Moragues, D. Otero, M. L. Pérez, A. N. Proto, J. J. Rossi, and W. Scheuer, *Phys. Rev. C* **9**, 299 (1974).

<sup>10</sup>*Table of Isotopes*, 7th ed. edited by C. M. Lederer and V. S. Shirley (Wiley Interscience, New York, 1978).

<sup>11</sup>H. Huck, M. L. Pérez, and J. J. Rossi (unpublished).

<sup>12</sup>D. R. Bes and R. A. Broglia, *Phys. Rev. C* **3**, 2349 (1971).

<sup>13</sup>D. R. Bes, R. A. Broglia, G. G. Dussel, R. J. Liotta, and B. R. Mottelson, *Phys. Lett.* **52B**, 253 (1974).

<sup>14</sup>K. Heyde, J. Sau, and R. Chery, *Phys. Rev. C* **16**, 2437 (1977).